BENDING FATIGUE OF WOOD: STRAIN ENERGY-BASED FAILURE CRITERION AND FATIGUE LIFE PREDICTION

Atsushi Watanabe
Graduate Student
E-mail: watanabe-atsushi@dmail.daiken.co.jp

*Yasutoshi Sasaki**
Professor
E-mail: ysasaki@nagoya-u.jp

Mariko Yamasaki
Associate Professor
Laboratory of Timber Engineering
Department of Biosphere Resources
Nagoya University
464-8601 Nagoya, Japan
E-mail: marikoy@agr.nagoya-u.ac.jp

(Received August 2013)

Abstract. In this study, bending fatigue behavior of Japanese cedar and Selangan batu was examined. A nonreversible triangular waveform with loading frequencies of 0.5 and 5 Hz was used as load. Applied loads were about 110-70% of the static strength. The fatigue life of Japanese cedar was found to be longer at 5 Hz, especially at low stress level. For Selangan batu, however, loading frequency did not affect fatigue life. When fatigue life exceeded about 40,000 cycles, a crack formed on the compressive sides of the specimens regardless of the loading frequency and species. Cumulative strain energy at failure was found to be the failure criterion regardless of the loading frequency. This criterion could be estimated using the strain energy through the static test. A fatigue life prediction method based on the strain energy of the second loading cycle was proposed. This prediction method provided a good prediction of fatigue life.

Keywords: Fatigue, strain energy, failure criterion, fatigue life prediction.

INTRODUCTION

Wood is a common construction material used all over the world. Structural wood is subjected to repeated cyclic stress during use and, in particular, during typhoons, earthquakes, and human movement. Long-term cyclic stress causes material fatigue. Therefore, many studies on the fatigue of wood and its composites, which are viscoelastic materials, have already been conducted. The effect of loading conditions, in other words, the loading frequency and waveform, on the fatigue behavior has been investigated. Previous studies reported that fatigue life extended at higher loading frequencies for solid wood under tension (Okuyama et al 1984), compression (Okuyama et al 1984; Clorius et al 2000), and torsion (Ando et al 2005) and for wood composites under bending (Thompson et al 1996) and shear through thickness (Sugimoto and Sasaki 2006). Marsoem et al (1987) and Gong and Smith (2003) compared triangular, sinusoidal, and square waveforms and found that the square waveform was the most damaging and the triangular waveform was the least damaging. Kohara and Okuyama (1992) and Gong and Smith (2003) reported that square waveforms became more damaging with increasing duty ratio, which corresponded

* Corresponding author

to the ratio of the loading time per cycle to total time per cycle.

Fatigue tests generally show a hysteresis loop for each loading cycle for wood and its composites. The area enclosed in the hysteresis loop corresponds to the dissipated strain energy or energy loss. Energy loss is considered to reflect fatigue damage (Okuyama et al 1984). The fatigue failure criterion based on energy loss was proposed independent of loading waveform (Kohara and Okuyama 1994a) and frequency (Clorius et al 2000). Other studies have investigated fatigue behavior on the basis of energy loss (Hacker and Ansell 2001; Pritchard et al 2001; Sasaki et al 2005). Strain energy also has been investigated in terms of fatigue for wood and its composites. Kohara and Okuyama (1994b) studied tensile fatigue of six species and investigated the relationship between energy loss during fatigue tests and strain energy during static tests. They proposed that the energy loss behavior during fatigue tests could be estimated using the strain energy obtained through static tests. Sugimoto et al (2007a) studied fatigue of plywood under shear through thickness under three loading conditions and analyzed its strain energy through fatigue tests. They showed that although the fatigue life depended on loading conditions, the fatigue behavior could be represented by strain energy regardless of the loading frequency and waveform. However, there are few studies on fatigue behavior of wood and wood components based on strain energy. Therefore, it is necessary to investigate fatigue behavior based on strain energy using other loading modes and materials. The purpose of this study was to investigate the bending fatigue behavior of softwood and hardwood based on strain energy.

MATERIALS AND METHODS

Specimen Preparation

Materials used in this experiment were Japanese cedar (*Cryptomeria japonica*), which is a softwood, and Selangan batu (*Shorea* spp.), which is a hardwood. These two species have widely different characteristics. Japanese cedar is light and soft, whereas Selangan batu is heavy and hard (Table 1). Clear specimens were processed from air-dried lumber samples of the selected timber species. Japanese cedar specimens (340 × 50 × 20 mm) were obtained from ten 2000 × 120 × 20-mm laminae. Selangan batu specimens (310 × 100 × 16 mm) were obtained from fifteen 2000 × 100 × 20-mm laminae. Specimen number (n), moisture content, and air-dried density (ρ_{air}), determined through static tests, are listed in Table 1.

Static Test

A static bending test was first performed before the fatigue test to determine the static strength of 20 Japanese cedar and 15 Selangan batu specimens. A midspan test (Japanese Industrial Standards 2009) was carried out under controlled conditions using an EHF-UB5-10L electro hydraulic servo testing machine (Shimadzu Corporation, Kyoto, Japan) with a span value set to 14 times the specimen thickness and a constant displacement rate. Actuator load and deflection were recorded using a dynamic PCD-320A data logger (Kyowa Electronic Instruments Co., Ltd., Tokyo, Japan).

Static test measurements provided modulus of rupture (MOR), modulus of elasticity (MOE),

Table 1. Static bending test results and specimen properties.[a]

Species	n		MC (%)	ρ_{air} (kg/m^3)	MOR (MPa)	MOE (GPa)	V_{static} (kJ/m^3)	TM
Japanese cedar	20	Mean	11.3	355	57.8	7.25	345	0.652
		COV (%)	4.80	7.16	12.3	14.4	28.6	6.60
Selangan batu	15	Mean	12.0	842	140	16.7	1080	0.694
		COV (%)	4.43	4.21	6.51	12.4	14.2	4.32

[a] n, number of specimens; MC, moisture content; ρ_{air}, air-dried density; MOR, modulus of rupture; MOE, modulus of elasticity; V_{static}, strain energy; TM, Tetmajer's coefficient; COV, coefficient of variation. V_{static} and TM were evaluated from strain values calculated using deflections, assuming that the specimen deforms like a circle.

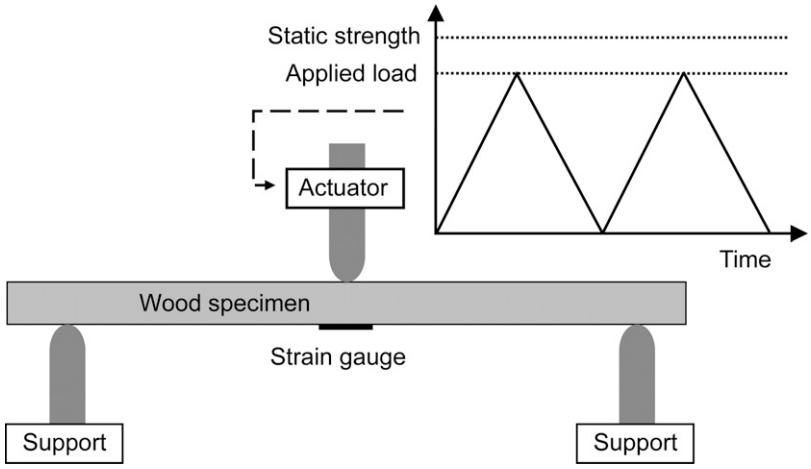

Figure 1. Loading method and waveform for fatigue test.

strain energy (V_{static}), and Tetmajer's coefficient (TM) for each specimen. MOR was evaluated from the maximum applied load. MOE was evaluated using 10-40% of the slope of the maximum applied load, which was approximated as the linear region of the stress–strain curves. V_{static} was evaluated using the area delimited by the stress–strain curve and the horizontal axis before reaching the maximum load. TM, which indicates specimen tenaciousness, was determined by dividing V_{static} by product of the maximum load and the strain. The MOR, MOE, V_{static}, and TM (Table 1) obtained for Japanese cedar and Selangan batu were analyzed statistically. These values were significant at a 1% level. F-test and Student's and Welch's t-tests were performed to compare Japanese cedar and Selangan batu. The tests showed that the MOR, MOE, V_{static}, and TM values between Japanese cedar and Selangan batu were significantly different at a 1% significance level.

Fatigue Test

Fatigue tests were conducted using the experimental set-up described for static testing. In addition, an axial strain gauge was attached to the specimen surface, which was subjected to tensile stress. The strain was recorded using the dynamic PCD-300A data logger (Kyowa Electronic Instruments Co., Ltd., Tokyo, Japan). A cyclic nonreversible triangular bending load was applied to the test specimen at loading frequencies of 0.5 and 5 Hz and was kept constant throughout the fatigue test. Loading method and waveform for fatigue tests are shown in Fig 1. The stress level was determined as the ratio between applied load and specimen static strength. The applied stress level ranged between about 110 and 70%. Ten Japanese cedar and 16 Selangan batu specimens were tested for each loading frequency. The data sampling frequency was adjusted to 100 Hz for the 0.5-Hz loading frequency and 500 Hz for the 5-Hz loading frequency.

RESULTS AND DISCUSSION

Relationship between Stress Level and Fatigue Life

Figure 2 shows the *S–N* diagram obtained by fatigue tests for all specimens. The semilogarithmic diagram shows a plot of the stress level against the number of cycles to failure (N_f), which represents the fatigue life. The linear–logarithmic relationship between stress level and fatigue life was found to be negative for all test conditions. The fatigue life of Japanese cedar was found to be longer at a loading frequency of 5 Hz than at 0.5 Hz, especially at low stress level (Fig 2a). Previous studies have

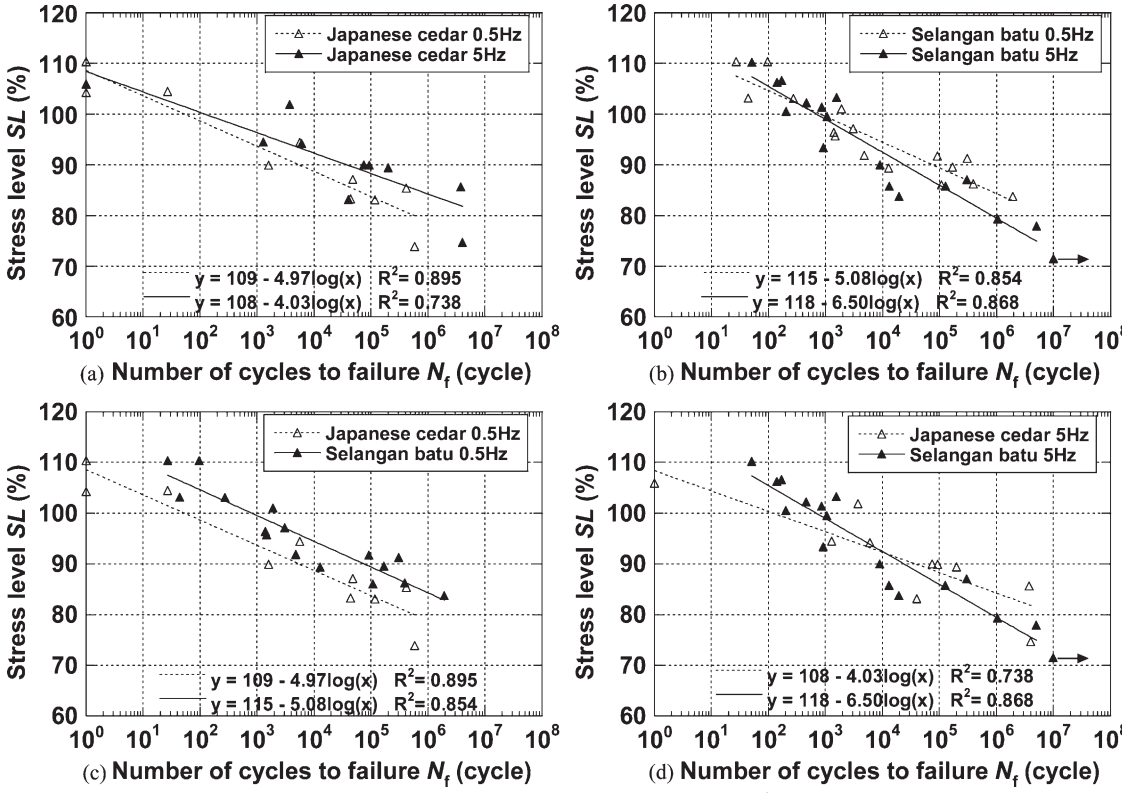

Figure 2. *S–N* diagrams. For Selangan batu, fatigue failure did not occur for 10^6 loading cycles at a loading frequency of 5 Hz and a stress level of 71%.

shown that the fatigue life of wood and its composites was longer at higher loading frequencies, as mentioned in the Introduction (Okuyama et al 1984; Thompson et al 1996; Clorius et al 2000; Ando et al 2005; Sugimoto and Sasaki 2006). Some studies reported that the loading frequency dependence of the fatigue life was affected by the stress level differently. Sugimoto and Sasaki (2006) showed that the fatigue life of plywood under cyclic shear through thickness using a triangular waveform was longer at a loading frequency of 5 Hz than at 0.5 Hz and that the difference in fatigue life became clearer with increasing stress level. Thompson et al (1996) also reported that the fatigue life of a chipboard with bending it at 0.015-0.15, 0.15-3.0, and 3.0-15.0 Hz was longer at higher frequencies. However, they found that the difference in fatigue life was more visible with decreasing stress level. The bending behavior of Japanese cedar shown here was the same as that for chipboard. The fatigue life of Selangan batu did not display any loading frequency dependence but may become shorter at 5 Hz at lower stress levels (Fig 2b). All regression lines in Fig 2 were statistically significant at the 1% significance level. The effects of loading frequency on the *S–N* diagrams were statistically examined through covariance analysis by checking the assumption of parallelism between regression lines (Otto and Longnecker 2000). Table 2 shows p values resulting for the two statistical tests. The statistical tests showed that there were no significant differences between the regression lines obtained at two different loading frequencies for stress levels of 110-70%. As previously mentioned, for lower stress levels, fatigue life may increase at higher loading frequencies.

Table 2. *P* values obtained for two statistical tests conducted on the regression lines shown in *S–N* diagrams.

Analyzed data	*P* value obtained by checking of the assumption of parallelism	*P* value obtained by ANCOVA[a]
Japanese cedar 0.5 Hz — Japanese cedar 5 Hz	0.370	0.099
Selangan batu 0.5 Hz — Selangan batu 5 Hz	0.117	0.223
Japanese cedar 0.5 Hz — Selangan batu 0.5 Hz	0.895	<0.001[b]
Japanese cedar 5 Hz — Selangan batu 5 Hz	0.028	0.950

[a] ANCOVA, covariance analysis.
[b] Significant at 1% level.

The difference in the fatigue life between Japanese cedar and Selangan batu was investigated for the same loading frequency. At 0.5 Hz, the fatigue life of Selangan batu was found to be longer than that for Japanese cedar (Fig 2c). In contrast, the fatigue lives of Japanese cedar and Selangan batu were found to be almost the same at 5 Hz (Fig 2d). *P* values (Table 2) showed that differences between regression lines were significant at the 1% significance level at 0.5 Hz but not at 5 Hz. The fatigue performance of Selangan batu was, therefore, slightly superior to that of Japanese cedar. Two reasons may explain this result. The first reason is the loading speed. As mentioned in the Introduction, previous studies have shown that the fatigue life was extended at high loading frequencies, thus at high loading speeds. Loading frequencies of 0.5 and 5 Hz corresponded to loading speeds of about 57.8 and 578 MPa/s, respectively, for Japanese cedar and 140 and 1400 MPa/s, respectively, for Selangan batu at a stress level of 100%. The loading speed of Selangan batu was 2.42 times as high as that of Japanese cedar for the same loading frequency. The fatigue life of Selangan batu was, therefore, longer than that for Japanese cedar because of its higher loading speed. The second reason is the tissue structure. Fatigue failure is caused by minor crack propagation, which may stop at interfaces between different tissues. Compared with Japanese cedar, Selangan batu, a hardwood, is composed of a greater variety of tissues, often interrupting microcrack propagation and extending fatigue life.

Failure Mode

Figure 3 shows the typical failure modes of Japanese cedar and Selangan batu in fatigue tests for long and short fatigue lives. The compressive sides of the specimens were found to differ depending on the fatigue life. They displayed a crack that was visible to the naked eye at long fatigue lives (Figs 3a and c) but no crack at short fatigue lives (Figs 3b and d). As discussed by Kohara et al (1997), the existence of this crack may be explained by the production of tensile stress on the compressive side in the unloading process of the fatigue test. When the load was applied to the wood and the microbuckling on the compressive side in bending appeared, the stress–strain relationship became tensile–compressive asymmetry, which produced slight tensile stress on the compressive side in unloading. Figure 4 shows the relationship between the existence of the crack and fatigue life (N_f). Points appearing in the upper part of the graph represent specimens with cracks visible to the naked eye, whereas points shown in the lower side correspond to specimens without a crack.

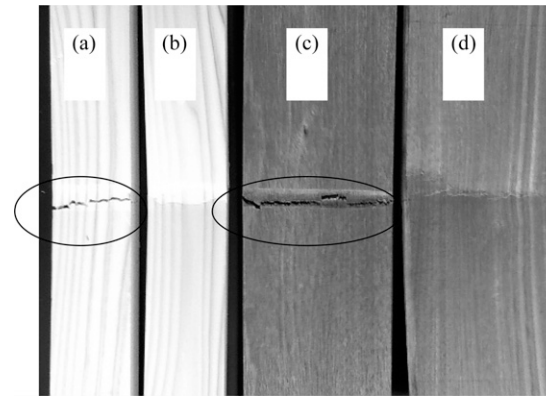

Figure 3. Typical bending fatigue failure modes observed on the compressive side: (a) Japanese cedar with a long fatigue life; (b) Japanese cedar with a short fatigue life; (c) Selangan batu with a long fatigue life; (d) Selangan batu with a short fatigue life.

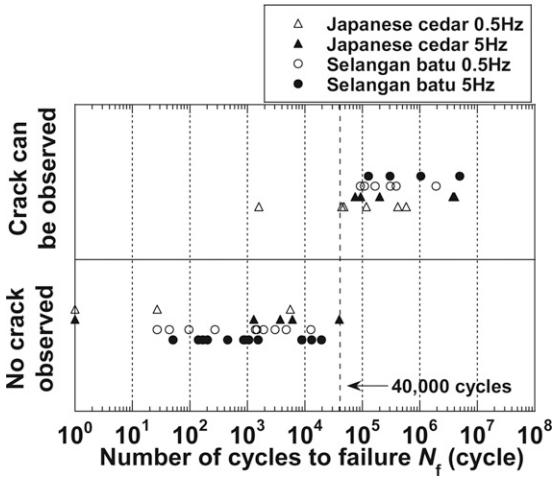

Figure 4. Appearance of cracks on the compressive side of the specimen.

The graph showed two very distinct populations depending on the fatigue life. The boundary between the two populations was found at a fatigue life of about 40,000 cycles regardless of the loading frequency and species. In this regard, Sugimoto and Sasaki (2006) proposed two models for the fatigue failure process depending on the stress level. At high stress levels, a minor crack generated in a microregion of a material causes the material to break immediately, leading to a little cumulative damage at failure. Conversely, at low stress levels, a few minor cracks do not cause material failure in the initial fatigue phase. Minor cracks are generated in the entire material, and a large accumulation of these minor cracks leads to fatigue failure, resulting in significant cumulative damage at failure. According to the first model, for a short fatigue life or at a high stress level, a minor crack generated in a microregion of the specimen caused it to break before a crack appeared on the compressive side. For a long fatigue life or at a low stress level, minor cracks were generated across the entire specimen, resulting in the appearance of a crack on the compressive side of the specimen.

Stress–Strain Curves

Figure 5 shows typical stress–strain curves at a loading frequency of 0.5 Hz for different loading cycle numbers (N) through a fatigue test. The overall slopes of the stress–strain curves decreased gradually with increasing loading cycle numbers, consistent with a decrease in bending rigidity. Also, residual strain increased regardless of the species and stress level. At low stress levels, the slopes of the initial rises of the stress–strain curves decreased more quickly than the overall slopes when the number of cycles increased (Figs 5b and d). This behavior originated from the formation of the crack on the compressive side of the specimen with increasing loading cycle numbers (Figs 3a and c). This crack significantly deformed the specimen. As the applied load increased, the crack closed up and the deformation of the specimen became smaller than when the crack remained open. A similar increase in residual strain, concomitant with a decrease in bending rigidity, was also observed at a loading frequency of 5 Hz for Japanese cedar and Selangan batu. The slopes of the initial rises of the stress–strain curves also decreased significantly at 5 Hz.

Changes in Bending Rigidity

The gradual decrease in the overall slopes of the stress–strain curves with increasing loading cycle numbers was investigated in detail. Changes in bending rigidity are shown in Fig 6 for increasing loading cycle numbers. The bending rigidity was evaluated using 30-70% of the slope of the maximum applied load, which was approximated as the linear region of the stress–strain curves (Fig 5). Figure 6 shows the semilogarithmic plot of the bending rigidity retention, which is the bending rigidity at each loading cycle normalized by that at the first loading cycle, as a function of loading cycle number (N). The change in bending rigidity depended on the stress level but not on the loading frequency. At low stress levels, the bending rigidity of Japanese cedar maintained a quasi-constant value from the first loading cycle to just before the fatigue life and decreased rapidly thereafter. Similarly, the bending rigidity was quasi-constant from the first loading cycle to just before the fatigue life before decreasing rapidly at high stress levels.

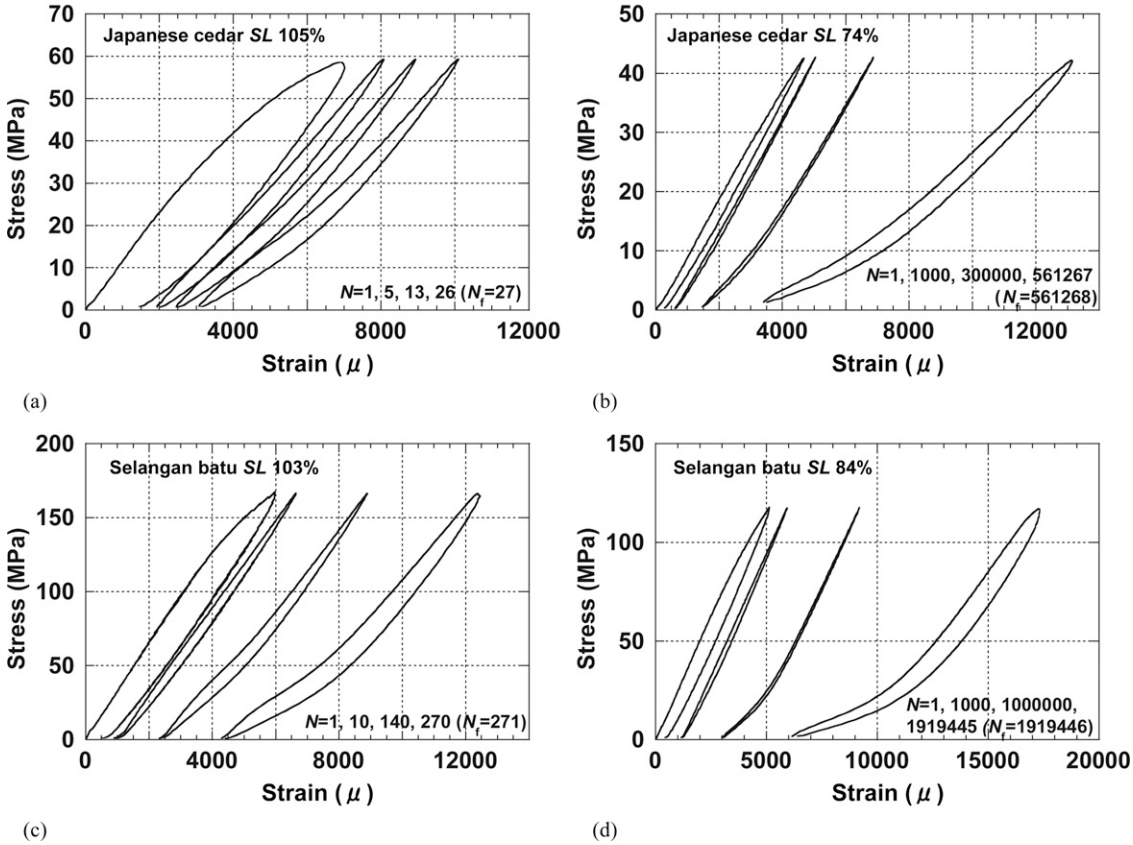

Figure 5. Typical stress–strain curves during the fatigue test at a loading frequency of 0.5 Hz (SL, stress level).

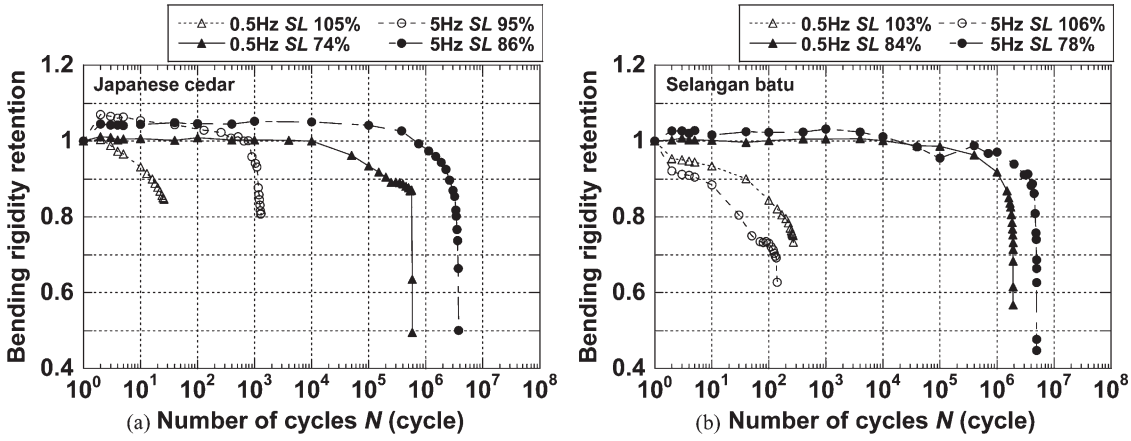

Figure 6. Changes in bending rigidity retention per cycle (SL, stress level).

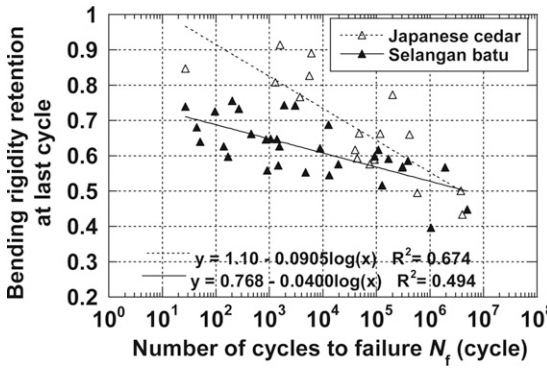

Figure 7. Relationship between bending rigidity retention of the last cycle and fatigue life.

However, the bending rigidity of the last cycle at high stress levels was greater than at low stress levels. At high stress levels, the bending rigidity of Selangan batu decreased significantly at the beginning of the test, especially between the first and second loading cycles. Otherwise, the changes in bending rigidity were the same for Selangan batu as for Japanese cedar. In other words, the bending rigidity remained at a certain value from the first loading cycle to just before the fatigue life and decreased rapidly thereafter. The bending rigidity of the last cycle was larger at high stress levels than at low stress levels. This difference in bending rigidity was investigated in detail. Figure 7 shows the relationship between the bending rigidity retention of the last cycle and fatigue life regardless of the loading frequency. The linear–logarithmic relationship between the bending rigidity retention of the last cycle and fatigue life was negative for Japanese cedar and Selangan batu. This result can also be explained using the fatigue failure model previously discussed (Sugimoto and Sasaki 2006). For a short fatigue life, the cumulative damage at failure was little, preventing the bending rigidity from decreasing significantly. The regression lines were statistically significant at the 1% significance level for Japanese cedar and Selangan batu. The effects of species on the regression lines were statistically examined by checking the assumption of parallelism. Significant differences were found between the regression lines at the 1% significance level (p value < 0.001). The bending rigidity retention of the last cycle was lower for Selangan batu than for Japanese cedar, especially at a short fatigue life. The difference in bending rigidity retention at the last cycle arises from the difference in tenaciousness (TM) between the species (Table 1). High tenaciousness means high resistance to crack propagation. Therefore, the high tenaciousness of Selangan batu stops the specimens from breaking immediately from a minor crack, suggesting that Selangan batu specimens require a large amount of minor cracks to fail.

Changes in Strain Energy

The area delimited by the loading curve and the horizontal axis in stress–strain diagrams is the strain energy per cycle (V_c), which corresponds to the energy conserved in the specimen per cycle. The semilogarithmic plot of the strain energy per cycle as a function of loading cycle numbers is shown in Fig 8. Changes in strain energy were found to depend on the stress level for the first loading cycle but not on the loading frequency. At high stress levels, the strain energy of the first loading cycle was much higher than that for the second loading cycle. This result may be explained as follows. The strain increases proportionally to the load applied to the specimen until a proportional limit is reached. Beyond this proportional limit, plastic strain, which is generally larger than elastic strain, is caused by breaking weak portions of the specimen or by buckling cell walls and destroying the tissue. During the first loading cycle, plastic strain is caused by breaking weak portions. Plastic strain does not occur as easily during the second loading cycle, because the weak portions are already broken. Therefore, the total strain increment decreases in the second loading cycle compared with the first loading cycle, decreasing the strain energy. At a low stress level, plastic strain is negligible, because the stress is almost the proportional limit or less. In contrast, plastic strain is not negligible at a high stress level. Therefore, the higher the stress level, the more remarkable the difference in

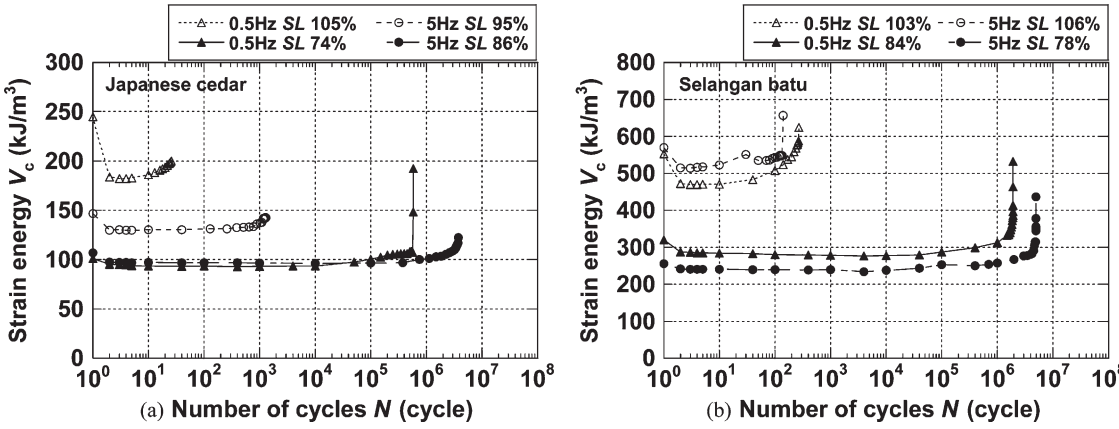

Figure 8. Changes in strain energy per cycle (SL, stress level).

strain energy between the first and the second loading cycles.

Except for the first loading cycle, changes in strain energy paralleled changes in bending rigidity, because strain energy increased with decreasing bending rigidity. The strain energy maintained a certain value from the second loading cycle to just before the fatigue life and then increased rapidly.

Cumulative Strain Energy at Failure

The sum of the strain energies from the first loading cycle to fatigue life is defined as the cumulative strain energy at failure (V_{acf}). Figure 9 shows the log–linear relationship between cumulative strain energy at failure and fatigue life (N_f). Quasi-similar relationships were found regardless of the loading frequency for the same species, suggesting that this relationship was the fatigue failure criterion for a given species. This result shows that fatigue failure did not occur for a given cumulative strain energy value and that specimens with long fatigue lives required a large cumulative strain energy to break. Specimens with greater cumulative strain energy displayed more damage such as a crack on the compressive side of the specimen (Figs 3a and c).

The cumulative strain energy at failure of Selangan batu was higher than that for Japanese cedar (Fig 9), because the strain energy applied to Selangan batu was greater than that for Japanese cedar. To exclude the influence of applied strain energy on the cumulative strain energy at failure, the cumulative strain energy at failure was normalized by the strain energy obtained through the static test (V_{static}). Figure 10 shows the relationship between the normalized cumulative strain energy at failure (V_{acf}/V_{static}) and fatigue life regardless of the loading frequency. The relationship was almost the same for all species. The regression line for Japanese cedar and Selangan batu was obtained as

$$V_{acf}/V_{static} = 0.654N_f^{0.942}\left(R^2 = 0.984\right) \quad (1)$$

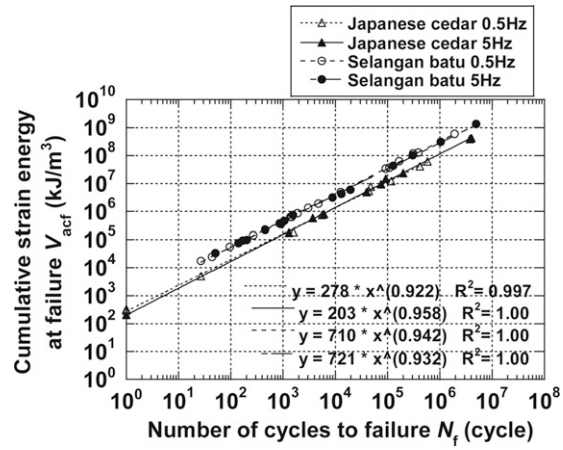

Figure 9. Relationships between cumulative strain energy at failure and fatigue life.

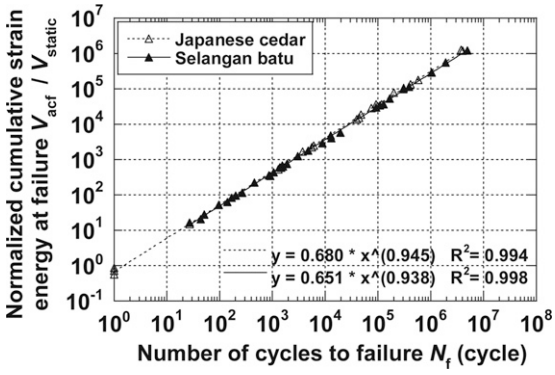

Figure 10. Relationships between normalized cumulative strain energy at failure and fatigue life.

Although Japanese cedar and Selangan batu were greatly different in air-dried density and static strength, their property could be expressed by Eq 1. Also, failure mode was the same independent of species (Figs 3 and 4). These results suggest that the relationship between normalized cumulative strain energy at failure and fatigue life may be expressed by Eq 1 regardless of the loading frequency and species for the nonreversible bending fatigue of wood. Kohara and Okuyama (1994b) studied the tensile fatigue of six species and proposed that the energy loss behavior during fatigue tests could be estimated using the strain energy obtained through static tests. Similar to the energy loss behavior, the cumulative strain energy at failure could also be estimated using Eq 1 and the strain energy in a static test.

Fatigue Life Prediction

Sugimoto et al (2007b) proposed a method to predict the fatigue life for various loading frequencies and waveforms using the cumulative strain energy at failure. However, their prediction method requires the strain energy to be determined through fatigue tests. A handier prediction method was, therefore, investigated.

As shown in Fig 8, the strain energy per cycle maintained a certain value from the second loading cycle to just before the fatigue life. Therefore, a certain value may have enormous influence on fatigue life. The relationship between this value, which was selected from the strain energy of the second loading cycle (V_{2nd}), and the fatigue life was investigated. To decrease individual variability, the strain energy of the second loading cycle was normalized by the strain energy obtained through the static test (V_{static}). Figure 11 shows the relationship between this normalized strain energy (V_{2nd}/V_{static}) and fatigue life (N_f). The relationship looked almost the same regardless of the loading frequency for the same species. The results of the log–linear regression for the data are listed in Table 3. Fatigue life prediction can be conducted using these regression lines and the normalized strain energy of the second loading cycle. To validate the fatigue life prediction method, the fatigue life of the specimens was predicted from the experimental data. The normalized strain energy of the second loading cycle at a given loading frequency was substituted with the regression line found at a different loading frequency to predict the fatigue life for the same species. For example, the fatigue life of Japanese cedar at 0.5 Hz was predicted using the regression line of Japanese cedar at 5 Hz and the experimental normalized strain energy of the second loading cycle for Japanese cedar at 0.5 Hz. The fatigue life of Selangan batu at 5 Hz was predicted from the regression line of Selangan batu at 0.5 Hz and the experimental normalized strain energy of the second loading cycle for Selangan batu at 5 Hz. Figure 12 shows the correlation between

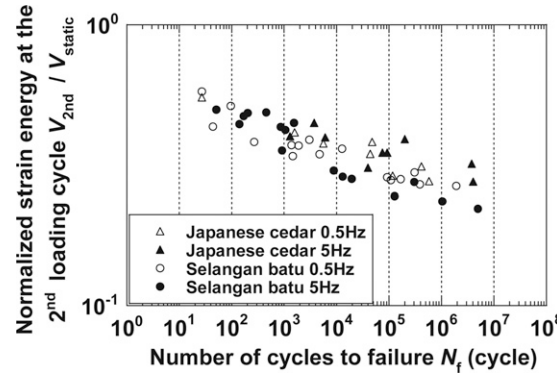

Figure 11. Relationships between normalized strain energy of the second loading cycle and fatigue life.

Table 3. Regression analysis results for the relationships between the normalized strain energy of the second loading cycle and fatigue life.

Species	Loading frequency	Regression line	Coefficients of determination R^2
Japanese cedar	0.5 Hz	$V_{2nd}/V_{static} = 0.676N_f^{-0.0640}$	0.935
	5 Hz	$V_{2nd}/V_{static} = 0.568N_f^{-0.0419}$	0.611
Selangan batu	0.5 Hz	$V_{2nd}/V_{static} = 0.601N_f^{-0.0613}$	0.838
	5 Hz	$V_{2nd}/V_{static} = 0.699N_f^{-0.0802}$	0.886

predicted ($p - N_f$) and experimental fatigue lives (N_f) in a logarithmic plot. The closer to the solid line, which represents y = x, the points are, the lower the errors are. All plots were found to lie almost on the solid line (Fig 12), suggesting that this method could predict the fatigue life well.

CONCLUSIONS

Bending fatigue tests were conducted for Japanese cedar and Selangan batu, and the effects of species, loading frequency, and stress level on the fatigue behavior were discussed. In addition, an approach to predict the fatigue life was investigated on the basis of the analysis of strain energy. The following conclusions were obtained:

1) The linear–logarithmic relationship between stress level and fatigue life was negative under all test conditions. The fatigue life of Japanese cedar appeared to increase at higher loading frequency, especially at low stress level. The loading frequency did not affect the fatigue life of Selangan batu. The fatigue performance of Selangan batu was found to be slightly superior to that of Japanese cedar.
2) For fatigue lives of more than about 40,000 cycles, a crack formed on the compressive side of specimens regardless of the species and loading frequency. The cause of the fatigue failure process is different depending on the fatigue life.
3) The bending rigidity was quasi-constant from the first loading cycle to just before the fatigue life and then decreased rapidly. The bending rigidity of the last cycle decreased with increasing fatigue life for both species, especially for Selangan batu. This difference between the species arises from the high tenaciousness of Selangan batu.
4) The strain energy of the first loading cycle was higher than that for the second loading cycle. The strain energy was almost constant between the second loading cycle and the cycle preceding the fatigue life and then increased rapidly. The cumulative strain energy at failure could be estimated from the strain energy obtained through the static test. This strain energy was found to be the fatigue failure criterion regardless of the loading frequency for the same species.
5) The fatigue life prediction method using the strain energy of the second loading cycle could predict fatigue life well.

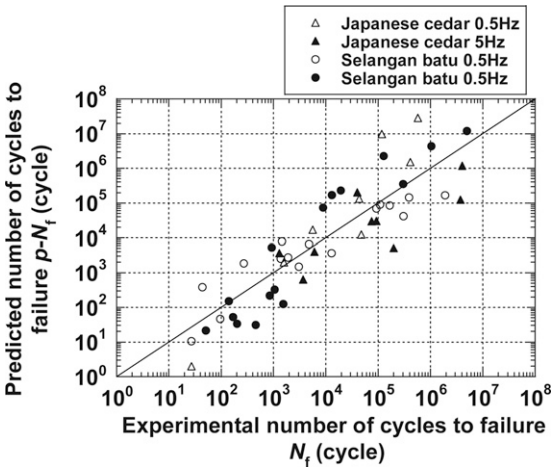

Figure 12. Correlation between predicted and experimental fatigue lives.

REFERENCES

Ando K, Yamasaki M, Watanabe J, Sasaki Y (2005) Torsional fatigue properties of wood (in Japanese). Mokuzai Gakkaishi 51:98-103.

Clorius CO, Pederson MU, Hoffmeyer P, Damkilde L (2000) Compressive fatigue in wood. Wood Sci Technol 34:21-37.

Gong M, Smith I (2003) Effect of waveform and loading sequence on low-cycle compressive fatigue life of spruce. J Mater Civ Eng 15:93-99.

Hacker CL, Ansell MP (2001) Fatigue damage and hysteresis in wood–epoxy laminates. J Mater Sci 36:609-621.

Japanese Industrial Standards (2009) JISZ2101. Method of test for wood. JIS, Tokyo, Japan.

Kohara M, Kanayama K, Nakai A, Nagata K, Okuyama T (1997) Damages in wood beams caused by fatigue under pulsating loads (in Japanese). Mokuzai Gakkaishi 43:909-915.

Kohara M, Okuyama T (1992) Mechanical responses of wood to repeated loading V—Effect of duration time and number of repetitions on the time to failure in bending (in Japanese). Mokuzai Gakkaishi 38:753-758.

Kohara M, Okuyama T (1994a) Mechanical responses of wood to repeated loading VII—Dependence of energy loss on stress amplitude and effect of wave forms on fatigue lifetime. Mokuzai Gakkaishi 40:491-496.

Kohara M, Okuyama T (1994b) Mechanical responses of wood to repeated loading VIII—Variation of energy loss behaviours with species. Mokuzai Gakkaishi 40: 801-809.

Marsoem SN, Bordonné PA, Okuyama T (1987) Mechanical responses of wood to repeated loading II—Effect of wave form on tensile fatigue. Mokuzai Gakkaishi 33:354-360.

Okuyama T, Itoh A, Marsoem SN (1984) Mechanical responses of wood to repeated loading I—Tensile and compressive fatigue fractures. Mokuzai Gakkaishi 30:791-798.

Otto LR, Longnecker MT (2000) An introduction to statistical methods and data analysis. Duxbury, North Scituate, MA, pp 943–974.

Pritchard J, Ansell MP, Thompson RJH, Bonfield PW (2001) Effect of two relative humidity environments on the performance properties of MDF, OSB, and chipboard. Part 2. Fatigue and creep performance. Wood Sci Technol 35:405-423.

Sasaki Y, Yamasaki M, Sugimoto T (2005) Fatigue damage in wood under pulsating multiaxial-combined loading. Wood Fiber Sci 37:232-241.

Sugimoto T, Sasaki Y (2006) Effect of loading frequency on fatigue life and dissipated energy of structural plywood under panel shear load. Wood Sci Technol 40:501-515.

Sugimoto T, Sasaki Y, Yamasaki M (2007a) Fatigue of structural plywood under cyclic shear through thickness I—Fatigue process and failure criterion based on strain energy. J Wood Sci 53:296-302.

Sugimoto T, Sasaki Y, Yamasaki M (2007b) Fatigue of structural plywood under cyclic shear through thickness II—A new method for fatigue life prediction. J Wood Sci 53:303-308.

Thompson RJH, Bonfield PW, Dinwoodie JM, Ansell MP (1996) Fatigue and creep in chipboard. Part 3. The effect of frequency. Wood Sci Technol 30:293-305.